JOURNAL OF MATERIALS SCIENCE 35 (2000) 4393–4404

On the influence of alloying elements on the bainite reaction in low alloy steels during continuous cooling

J. WANG
Netherlands Institute for Metals Research, Rotterdamseweg 137, 2628 AL Delft, The Netherlands
E-mail: j.wang@TNW.tudelft.nl

P. J. VAN DER WOLK
Delft University of Technology, Rotterdamseweg 137, 2628 AL Delft, The Netherlands

S. VAN DER ZWAAG
Delft University of Technology, Rotterdamseweg 137, 2628 AL Delft, The Netherlands

The CCT diagrams of a class of Fe-(0.1–0.6)C-(0.4–2.0)Si-(0.4–2.0)Mn-(0.5–2.0)Cr-(0.0–0.8)Mo steels are predicted by an artificial neural network (ANN) model. The results indicate that an increase in carbon concentration (C wt%) gives rise to a decrease in bainite start (BS) temperature. The rate of decrease depends also on cooling rate. Additions of Si, Mn, Cr and Mo all decrease the bainite start temperature. The dependencies for different alloying elements vary: 32, 100–120, 100–130, and 70–150°C per wt% of Si, Mn, Cr and Mo, respectively. Mn shifts the whole bainite transformation region to the far right-hand side of the CCT diagram, while C, Cr, and Mo have considerable, and Si has minor effects on the incubation period of bainite. Mn and Cr significantly decrease the MS temperature, while Si only has a minor influence. When Mo $<$ 0.5 wt% it has a minor influence, whilst when Mo $>$ 0.5 wt%, it increases MS temperature. Quasi-isochronal and quasi-isothermal methods have been used to analyze the influence of the proportion of Mo to C upon the BS and incubation period. Attempts, for qualitative explanations using the shear and diffusion mechanism, as well as a certain amount of thermodynamic analysis, have been made to interpret the influence of alloying elements on the nucleation of the bainite reaction. The results support that bainite reaction takes place utilizing a diffusion-controlled mechanism.

1. Introduction

A study on bainite formation is attractive not only from a fundamental perspective but also because of its practical importance, as bainitic steels are a series of promising steel materials. Thus, it is worthwhile to study the effect of different alloying elements on the bainite reaction under continuous cooling rather than isothermal conditions [1, 2]. However, it is by no means trivial to derive the effects of alloying elements on the transformation kinetics of bainite formation from published continuous cooling transformation (CCT) diagrams directly, as few systematic studies on alloy dependence over a sufficiently wide concentration range exist. Hence, it is necessary to condense the scatted information from the multitude of CCT diagrams in a consistent model. Two fundamentally different modeling methods exist: physical [1, 3–6] and statistical. It is immediately clear that no proper physical model can be established unless the transformation mechanism has been completely understood. In addition, modeling a continuous cooling transformation is difficult because of the complexity involved with non-isothermal nature [3, 4, 7]. An artificial neural network (ANN) is an efficient tool to model a complex physical process [8]. Unlike a physical model, the ANN model is a statistical one that is usually based on a large amount of experimental CCT diagrams and accordingly the predicted results are directly related to the practical situation. There are some other statistical empirical models [9–11], yet most of them are based on a predefined linear influence of alloying elements on transformation temperatures. However, it is well known that the effects of a single alloying element do not necessarily scale linearly with its concentration. Now that nonlinear interactions between two or more elements can play an important role, it is difficult for specific empirical models to figure out various influences of alloying elements. Hence, the studies in this article are based on the CCT diagrams predicted by ANN [12]. The ANN CCT model itself is based upon the information contained in several

atlases of experimental CCT diagrams. An ANN model is superior to the usual empirical statistical models in that it introduces such a complicated function to describe the dependence of interphase boundary position upon alloy element concentration that it proves itself an efficient mathematical solution to any physical process [13]. When such an ANN model for bainite formation under linear or natural cooling is available, it can be used to examine and validate qualitative and semi-quantitative physical models for bainite formation.

The bainite reaction is one of the most interesting transformations in steels since it reassembles both the high temperature diffusional decomposition products (ferrite or pearlite), and the low temperature shear product (martensite) [14]. This duality, in return, gives rise to two different ideas on the mechanism of bainite reaction. The first is the shear or displacive mechanism [15], that is, bainite is formed in a similar way to martensite. What is different is that the bainite reaction may be accompanied more or less by the redistribution of carbon atoms between ferrite (α) and austenite (γ) at the nucleation stage and after the transformation [16].

Another principal concept regarding the bainite reaction is that the lattice of ferrite (b.c.c.) will be reconstructed by diffusion. The mobility of the α/γ interface depends on the volume diffusion of carbon inside austenite [16]. A local thermodynamic equilibrium of carbon is reached on the interface boundary, while no partitioning of substitutional alloying elements takes place throughout the transformation. Nevertheless, segregation of substitutional alloying elements may happen within the transient zone of the boundary, and give rise to the formation of a thin concentration spike in front of the moving interface, i.e., the so-called no-partition local equilibrium (NPLE) [17] rather than paraequilibrium condition. In this article, the influence of alloying elements on the nucleation of bainite will be analyzed utilizing these two different hypotheses.

2. Construction of ANN model and test alloys

2.1. Artificial neural network (ANN)

A wide variety of neural networks exist for various applications. The type used for this research is the hierarchical feedforward ANN [12] that is widely used for modeling. The network has twelve input parameters (austenitizing temperature, concentrations of C, Si, Mn, Cr, Cu, P, S, Mo, V, B, and Ni), one hidden layer with 12 nodes, and 128 output parameters, which are specified in Section 2.2 of this article. The architecture of the ANN used here is schematically shown in Fig. 1a. The training algorithm used is the momentum version of the backpropagation of error training rule [12] with a maximum of 10000 iterations, a learning rate of 0.5 and momentum term μ set for each iteration as a function of the residual standard deviation (RSD) of the training set. To prevent the network from overtraining, the data set is split into a training set containing 75% of the data and a validation set containing the remaining 25%. The training data have been selected using the Kennard-Stone algorithm [18], which has been used to maximize the variance of the compositional domain of

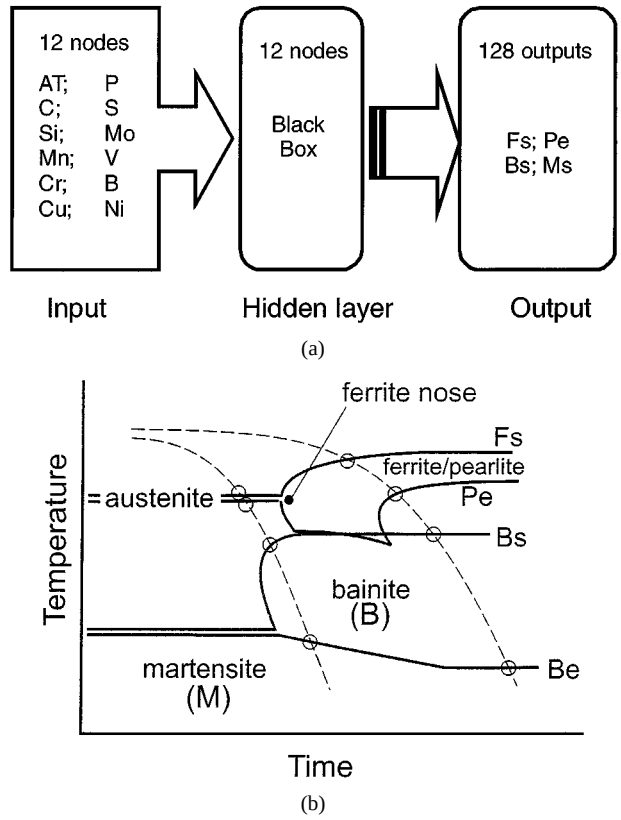

Figure 1 (a) Schematic architecture of the ANN model (b) Conversion scheme of CCT diagrams.

the training data. The weights determined after the iteration for which the error in the test set is at its minimum are used for the neural network model.

2.2. Data processing

The hierarchical and feed-forward ANN model is established based on 151 CCT diagrams. 87 are selected from a CCT diagram collection of a molybdenum steel company [19], and 64 from a collection of the VDEh [20]. The fact that most of the CCT diagrams incorporated into this model have a deep bay to separate proeutectoid ferrite and bainite transformations areas is helpful for this research. CCT diagrams need to be converted from a graphical into a numerical format. Several conversion schemes can be conceived [21]. The one used for this model is an intercept method, in which a set of fixed cooling rate curves are drawn over the diagram, as shown in Fig. 1b. The CCT diagram can be reconstructed by using the coordinates of the intercepts of these curves with the phase boundaries, which are determined by a pair of parameters, *Ts* and τ. An advantage of the intercept method above other methods is that the diagram can be represented by a relatively small number of data. The choice of linear cooling curves as test lines makes the model easily extendible with information such as the hardness reached on cooling, and the fraction of transformed material to be incorporated into this model. For this ANN model, 32 cooling curves with cooling rates ranging from 750 °C/s to 0.001 °C/s have been used to represent each CCT diagram. For each cooling curve, its intercepts with the upper ferrite/

TABLE I Composition of the database used by current ANN model (wt%)

Alloying Elements	C	Si	Mn	P	S	Ni	Cr	Mo	V
Lower Limit	0.09	0.08	0.29	0.00	0.00	0	0	0	0
Upper Limit	1.42	1.62	1.98	0.044	0.054	4.56	2.29	1.02	0.31
Reliability Range	0.10–0.60	0.15–1.55	0.5–1.5	<0.04	<0.03	<0.24	<1.55	<0.52	<0.11

TABLE II Composition list of all test alloys (wt%)

Code	C	Si	Mn	Cr	Mo	Code	C	Si	Mn	Cr	Mo
A1	0.10	0.40	0.80	1.00	0.00	B8	0.40	0.50	1.00	0.50	0.40
A2	0.20	0.40	0.80	1.00	0.00	B9	0.40	0.50	1.00	1.50	0.40
A3	0.30	0.40	0.80	1.00	0.00	B10	0.40	0.50	1.00	2.00	0.40
A4	0.40	0.40	0.80	1.00	0.00	B11	0.40	0.50	1.00	1.00	0.00
A5	0.50	0.40	0.80	1.00	0.00	B12	0.40	0.50	1.00	1.00	0.20
A6	0.60	0.40	0.80	1.00	0.00	B13	0.40	0.50	1.00	1.00	0.60
B1	0.40	0.50	1.00	1.00	0.40	B14	0.40	0.50	1.00	1.00	0.80
B2	0.40	1.00	1.00	1.00	0.40	B15	0.40	0.50	1.00	1.00	0.50
B3	0.40	1.50	1.00	1.00	0.40	B16	0.10	0.50	1.00	1.00	0.40
B4	0.40	2.00	1.00	1.00	0.40	B17	0.20	0.50	1.00	1.00	0.40
B5	0.40	0.50	0.50	1.00	0.40	B18	0.30	0.50	1.00	1.00	0.40
B6	0.40	0.50	1.50	1.00	0.40	B19	0.50	0.50	1.00	1.00	0.40
B7	0.40	0.50	2.00	1.00	0.40	B20	0.60	0.50	1.00	1.00	0.40

austenite boundary (FS), the lower pearlite/austenite boundary (PE), the upper bainite/austenite boundary (BS), and the lower bainite/austenite boundary (BE).* As a result, there are totally 128 output parameters of the network which are the intercept temperatures of FS, PE, BS, and BE with 32 predefined cooling curves. In this article, we only consider the bainite transformation area, which is generally associated with the BS and MS temperatures.

2.3. Test alloys

The composition ranges of alloying elements for the collected CCT diagrams are vitally important since they determine the validity and reliability of the ANN model. The upper and lower concentration limits of the relevant elements involved in this ANN model are given in Table I. The reliability of the ANN model is affected not only by the concentration range of a specific alloying element, but also by the frequency distribution of the CCT diagrams in the multi-dimensional concentration space. The reliable ranges of the alloy elements are also listed in Table I. More details on the concentration distribution frequency of this database have been described elsewhere [21].

In this article, two base alloys are selected. One is Fe-0.4C-0.4Si-0.8Mn-1.0Cr (Base A or A4), and another is Fe-0.4C-0.5Si-1.0Mn-1.0Cr-0.4Mo (Base B or B1). Starting from these base alloys, the effect of alloying elements can be studied by increasing the concentration of selected elements. In total, 26 alloys have been studied. Amongst them, 5 were derived from Base A, and are used to study the influence of C concentration and cooling rates. The C concentration of Class A steels ranges from 0.10 to 0.60 wt%. The remaining 19 are based on Base B, and are utilized to study the influence of the alloying elements of Si, Mn, Cr, Mo, and C. The composition ranges of class B steels are 0.10–0.60C, 0.50–2.00Si, 0.50–2.00Mn, 0.50–2.00Cr, and 0.00–0.80Mo wt%. The compositions of both Class A and Class B alloys mentioned above are listed in Table II. Note that the alloying elements chosen here are typical representatives of commonly used alloying elements in low alloy steels. According to their special properties, they are classified as carbide formers: Mn, Cr and Mo; non-carbide former: Si; ferrite stabilizers: Mo and Si; austenite stabilizer: Mn; again austenite stabilizer: Cr (depending on its concentration). These chemical properties of these alloying elements will be noticed in the discussion. The austenitizing temperature of steels Class A, i.e., A1 through A6, is 1050°C, and that of Class B, B1 through B20, is 950°C. It should be pointed out that a further examination has indicated that austenitizing temperature has minor influence on the shape and position of the CCT diagrams [21] probably because most of the steels have only one CCT diagram that was measured at a certain austenitizing temperature.

3. Results and discussion

3.1. Influence of C and cooling rates on bainite reaction

Fig. 2a shows the bainite transformation regions of CCT diagrams of Class A steels with the carbon concentration changing between 0.10 and 0.60 wt%. In this model, for numerical reasons, the BS temperature line has been artificially extended to very low cooling rates parallel to the time axis and to very high cooling rates along the MS line. Therefore, the predicted bainite reaction region at the lower and higher cooling rates should be disregarded, and only that at medium-cooling rates will be dealt with.

* Note that we define the BS temperature as the upper bainite/austenite boundary. It is different from the conventional definition of Bs. Clearly in Fig. 1b, the maximum BS equals to the conventional Bs. Additionally, the left part BE is extended along Ms temperature so that it equals to Ms under fast cooling conditions.

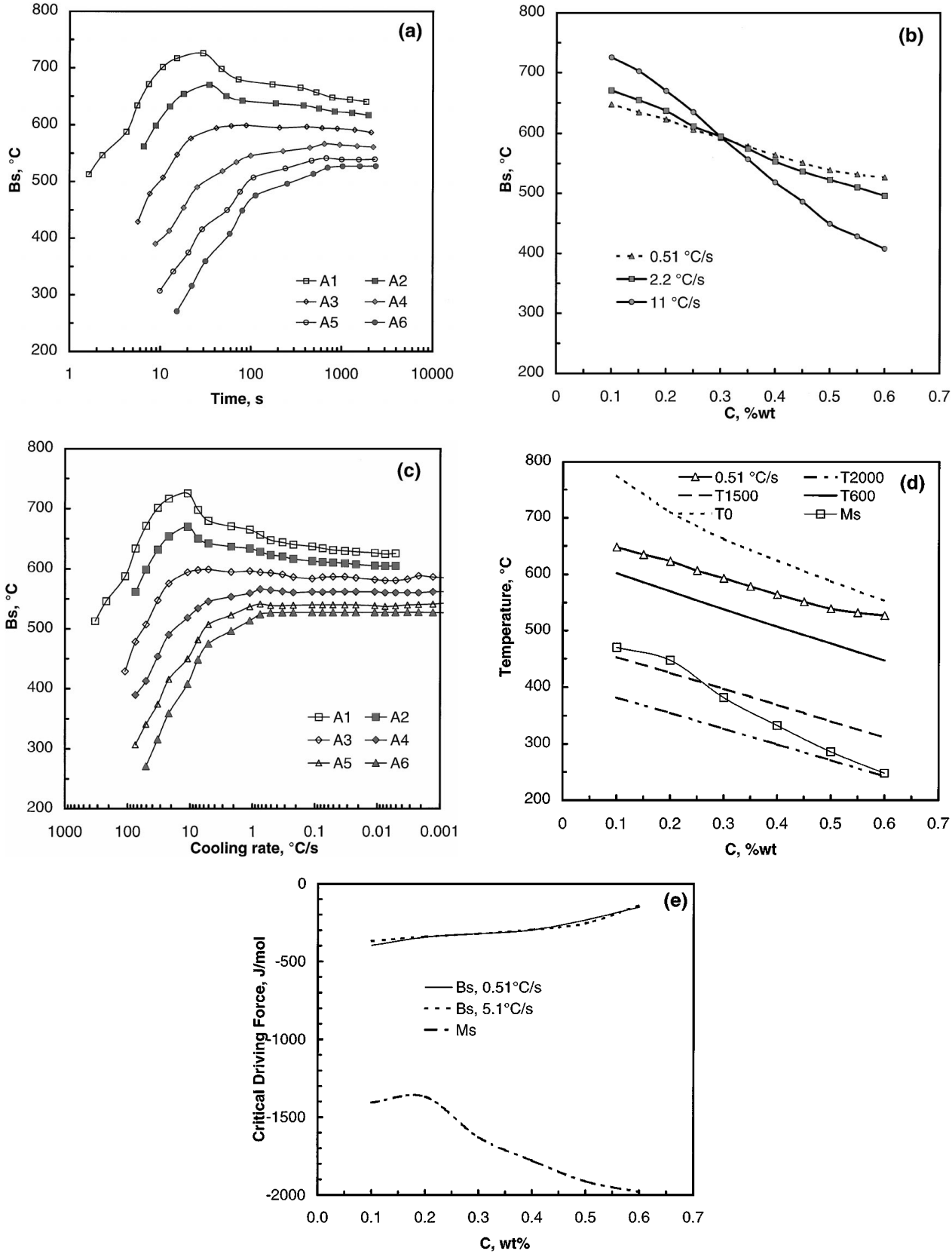

Figure 2 Influence of C and cooling rate in steels of Class A (a) BS versus time; (b) BS versus C concentration; (c) BS versus cooling rate; (d) comparison with thermodynamic calculation (number after T denoting driving force in J/mol); (e) critical driving force.

It is clear in Fig. 2a that the lines of the bainite start temperature are not C-shaped but hump-shaped. This should be attributed to the pre-bainite, namely ferrite or pearlite reaction. The volume diffusion controlled prebainite reactions are always accompanied by an increase of the carbon concentration in the retained austenite. Thus, the prebainite decomposition of austenite will retard the bainite reaction. Fig. 2a also indicates that if the carbon concentration of the steel is more than 0.3 wt%, the pre-bainite reactions have a weak influence on the bainite reaction. This is because the increase in carbon concentration would give rise

to the decrease in the amount of ferrite formed before bainite reaction. Correspondingly, the influence of the degree of ferrite reaction on the bainite reaction will decrease. Actually, by comparing the hump positions in Fig. 2a with the ferrite start temperature lines [22], we see that the peaks appear at the cooling rates corresponding to the ferrite noses.

Fig. 2a also illustrates that carbon tends to shift slightly the phase boundary of bainite and austenite towards the right side. This means that the addition of carbon will considerably prolong the incubation period of bainite reaction. Meanwhile, the BS lines will be significantly moved by C towards the bottom of Fig. 2a. As shown more clearly in Fig. 2b, where the carbon concentration is chosen as the x-axis, the decrease of BS temperature is inversely proportional to the increase of carbon concentration. This is understandable according to the lattice reconstruction transformation model since the more carbon in the austenite, the smaller the carbon concentration gradient inside the austenite grain in front of the transformation interface, or according to the shear mechanism because increase in carbon concentration gives rise to a decrease in the Gibbs energy difference between bainite and austenite.

In addition to the C concentration, the cooling rate exerts a strong influence on the bainite reaction, and the two effects are coupled too. The effect of cooling rate on BS is evident in Fig. 2a and b, and clearer in Fig. 2c. The decrease rates vary from 255, 360, to 676°C per wt% carbon at cooling rates of 0.51, 2.2 and 11°C/s, respectively. Fig. 2c further indicates that, in medium and high carbon steels, if the cooling rate is below 1°C/s, BS is more or less independent of the cooling rates. Above 1°C/s, however, an increased cooling rate will decrease the BS temperature. A wider comparison [22] indicates that the cooling rate has a similar influence on bainite and ferrite reactions. The difference is that in the case of ferrite reaction, the critical cooling rate is 0.1°C/s while that for bainite is 1°C/s. This immediately indicates that the bainite reaction is probably associated with thermally activated processes. If the activation energy is sensitive to alloy composition, the nucleation of bainite is bound to be controlled by diffusion. It is then more likely that the effect arises from the diffusion of carbon atoms rather than that of substitutional solutes. More details of the influence of alloying elements on the nucleation of bainite reaction will be explained later.

We will now try and link the predictions of the ANN model to physical models. Following earlier predictions on MS temperature [23], it is acceptable to define the critical driving force for athermal heterogeneous nucleation as 1500 to 2000 J/mol, but that during growth it may be as small as 600 J/mol [24]. The critical temperatures corresponding to various critical driving forces, the free energy difference between austenite and ferrite of the same composition [25], have been theoretically calculated. The free energy difference was calculated using MTDATA, commercial thermodynamics software package. The Gibbs energy was calculated assuming that there is only one phase, either f.c.c. austenite or b.c.c. ferrite (without tetragonality and ordering of carbon), present. For simplicity, no miscibility is assumed to exist in b.c.c. ferrite. The results are plotted in Fig. 2d. It is clear that the transformation of austenite into ferrite of the same composition has a smaller driving force than either that into equilibrium ferrite or that into martensite does [25]. One more line in Fig. 2d represents the dependence of T_0 on C concentration. The slope of BS is quite different from the slope of the T_0 line, and based on these data it seems unlikely that the conditions related to T_0 are related to those for bainite formation. Alternately, the T_0 does not define an upper temperature limit of BS for bainite reaction. Fig. 2d implies that BS tends to cross T_0 at the high level of C concentration. This was also observed in the Fe-C alloy [23].

Now, we focus on the qualitative and physical understanding of the influence of C concentration on the bainite reaction. The influence of C on the nucleation kinetics of bainite can be viewed in two ways. First, based on the shear model [15, 16], the onset of the bainite reaction is governed by the critical driving force, i.e. the Gibbs energy decrease of the closed system due to the formation of martensitic ferrite from austenite. The effect of carbon can be well explained utilizing the shear mechanism. It is evident that increase in carbon concentration gives rises to a decrease in the free energy difference between ferrite and austenite, i.e., the driving force for nucleation of bainite. Kaufman and Cohen [26] proposed that the nucleation of martensite in steels is heterogeneous. If bainite utilizes the similar nucleation mechanism, the rate of nucleation is controlled entirely by interfacial motion that is further determined by the activation energy for the formation and thermally activated motion of transformation dislocations [27]. In this case, the BS boundary will be physically related only to the Gibbs energy decrease. Supposing there is no carbon diffusion at the nucleation stage of bainite reaction, in other words, the composition of the bainitic ferrite nucleus has the same chemical composition as that of the nominal composition of the alloy (or the average composition of austenite), the critical driving force for athermal nucleation of bainite was calculated and presented in Fig. 2e. It indicates that the critical driving force for bainite nucleation under above assumption is within the range of 150 and 400 J/mol, and depends somewhat on the carbon concentration of the alloys. For comparison, the critical driving force for athermal nucleation of martensite is also plotted against C concentration in Fig. 2e. It is clear that the latter is about 5 times larger than the former. Note that the dependencies of the critical driving forces for bainite and martensite reactions on carbon concentration are different. In the case of martensite transformation, the critical driving force decreases first, then rises with increasing carbon concentration, yet in the case of bainite reaction, it decreases.

Back to Fig. 2d, we also see that the critical driving force for bainite is too small for shear (requiring around 600 J/mol) to proceed. One could suppose that in addition to interface motion activation, a certain degree of diffusion activation might be involved in bainite nucleation stage, which is normally associated with the volume diffusion or redistribution of carbon atoms since redistribution of substitutional atoms seems impossible

at the temperature of bainite reaction. This means the composition of the bainite nucleus is different from that of the nominal composition of the austenite. In this case, the nucleation driving for such a thermal activated nucleation process is different from those calculated in Fig. 2d, and can be determined with the Hillert method [28]. The evaluation of the diffusion-activated nucleation of bainite will be discussed elsewhere. It should be pointed out that if neither prebainite transformation occurs nor spinondal decomposition of austenite takes place (this has been proven to be thermodynamically impossible), the growth of such a bainitic nucleus would be inevitably controlled again by carbon diffusion, and this is in contradiction with the basic principle of the shear theory.

An alternative interpretation of bainite nucleation is based on the local equilibrium concept, in which the carbon concentration gradient is the effective driving force for bainite growth. Decrease in the driving force will definitely increase the time needed for carbon atoms to diffuse away from the interface, and in other words, inevitably decrease the kinetics of bainite growth [29]. The consistency of predicted results mentioned above with the diffusion controlled-mechanism is straightforward and thus not necessary to be extended in this article.

In addition to Class A steels, the influence of C on bainite reaction has also been examined for the Class B steels, which contains 0.40 wt% Mo leading to a gap separating the bainite reaction region from that of ferrite in a CCT diagram. Fig. 3a presents the austenite/bainite boundaries for the Class B alloys with different carbon concentrations. Compared with Fig. 2a, it is evident that the incubation time is increased while transformation temperature decreased. Also, the boundary lines lose the hump-shaped characteristics since Mo tremendously retards the prebainite reactions [22]. The influence of C concentration is further shown in Fig. 3b. Apparently, C reduces the BS temperature. The dependence depends on cooling rates, as illustrated in Fig. 3c. If the cooling rate is below 0.13°C/s, the BS seems to be independent of cooling rate. If the cooling rate is above 1.3°C/s, the BS decreases with increasing cooling rate. This means that there is a critical cooling rate of between 0.13 and 1.3°C/s, below which the reaction under continuous cooling is more or less the same as that under the isothermal cooling conditions.

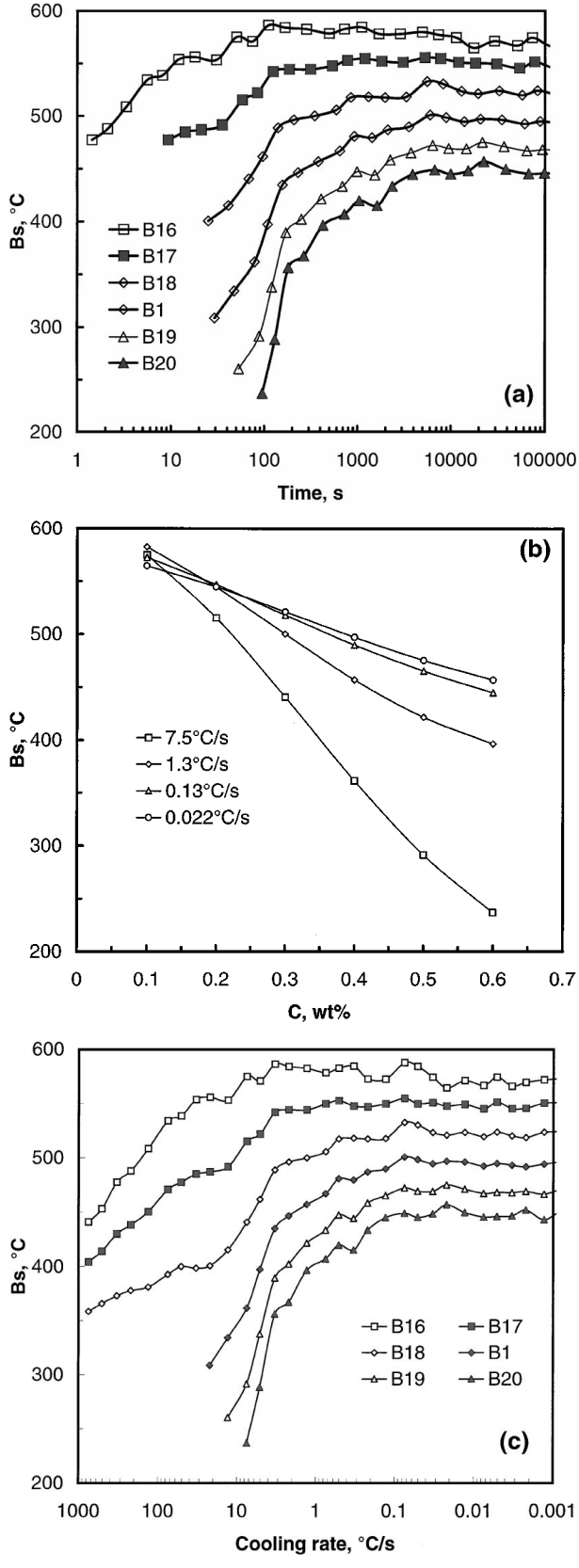

Figure 3 Influence of C on bainite start temperature in Class B steels (a) BS versus time; (b) BS versus C concentration; (c) BS versus cooling rate.

3.2. Influence of Si on bainite reaction

Fig. 4a shows the influence of silicon on the transformation kinetics of the bainite reaction. The statistical analysis clearly indicates that an increase in Si gives rise to a decrease of the BS temperature. In a word, Si is found to retard slightly the bainite reaction. The quantitative influence of Si on the BS temperature is given in Fig. 4b, where BS is plotted versus the Si concentration. Five curves in Fig. 4b correspond to cooling rates of 5.1, 3.3, 1.3, 0.33, 0.013°C/s. Except the lowest and highest cooling rates of 0.013 and 5.1 °C/s, the slopes of the curves are approximately the same, i.e., −33.3, −32.6 and −32.5, with an average of 32.8 ± 0.3°C per 1 wt% silicon. It is apparent that the effect of Si on BS is only a tenth of that of carbon.

Understanding the influence of Si on the bainite reaction is difficult [30] but rather important. If bainite forms by means of shear, no diffusion, partitioning, or segregation of Si atoms would take place in the course of bainite reaction. Thus, its growth kinetics depends

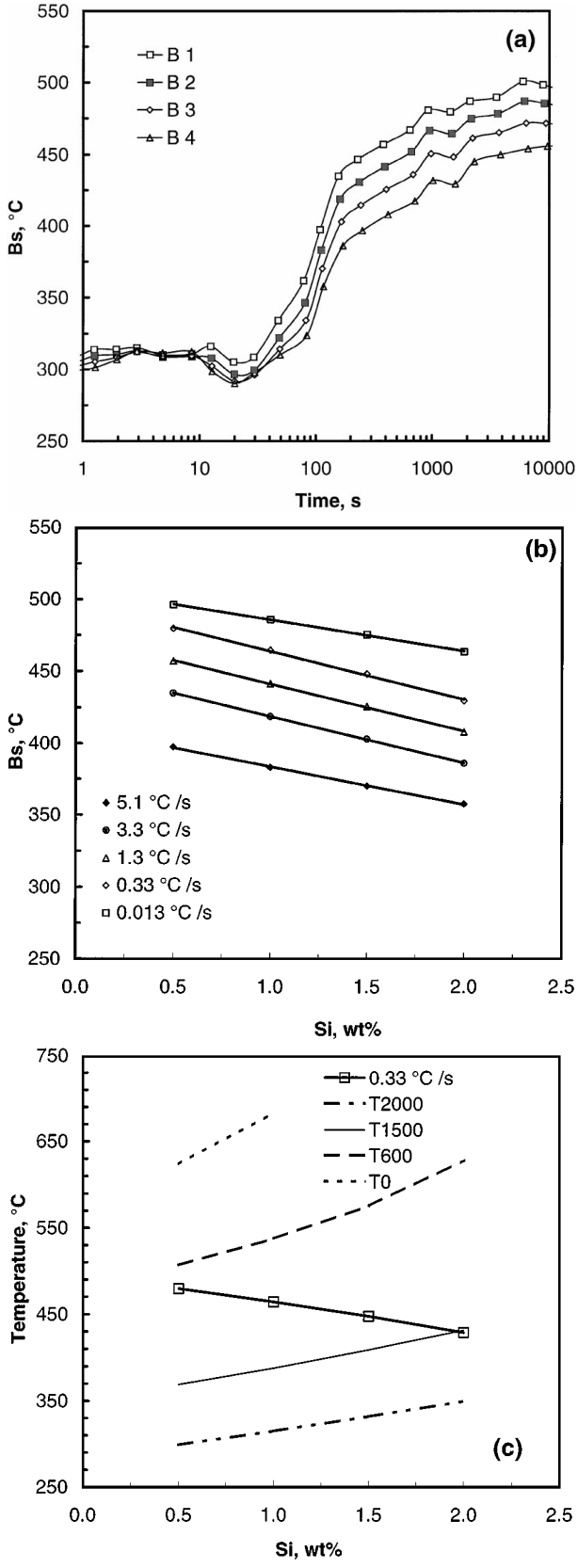

Figure 4 Influence of Si on bainite start temperature (a) BS versus time; (b) BS versus Si concentration; (c) compared with thermodynamic calculation by assuming different critical driving forces.

largely on the free energy difference between ferrite and austenite. Si is a weak ferrite stabilizer. It will decrease the free energy of ferrite, and thus increase the driving force for bainite reaction. The dependence of the free energy difference on Si concentration is implicitly shown in Fig. 4c. Apparently, all calculated lines in Fig. 4c have a positive slope, indicating that Si is expected to accelerate bainite reaction. This is in contradiction with the predicted results.

The left-hand sides of the bainite austenite boundaries in Fig. 4a actually represent the MS temperature of the steels. Compared with the critical driving force for heterogeneous nucleation, either by the Kaufman and Cohen model [26] or by the Olson and Cohen model [31, 32], the driving force decrease due to an increase of Si is too small to cause considerable change in MS temperature, and thus it is expected and apparently evident in Fig. 4a that Si has a minor influence on MS, as is indeed observed [33].

Now let us try to find the explanation from the diffusion mechanism theory. According to a microstructural definition, bainite is defined as the non-lamellar eutectoid decomposition product of austenite [16]. Therefore, the influence of the alloying elements on bainite reaction may be examined from two aspects: the influence of alloying elements on the formation of the bainitic ferrite, and the influence of alloying elements on the formation of bainitic carbide [34]. The normal carbide composing the bainitic structure in low alloy steels is cementite. If the growth kinetics of bainite is dominated by the ferrite component, as a typical non-carbide forming element, silicon itself does not change the true paraequilibrium state of the α/γ boundary [35], and accordingly is expected to have minor influence on the overall growth kinetics of bainite reaction. Considering the influence of Si on the activity of C, we might come to the same but apparently wrong conclusion. If the bainite reaction kinetics were affected more or less by the precipitation of carbide, however, silicon would possibly decrease the growth rate of bainite since Si is relatively insoluble in cementite. This means that the redistribution of Si is expected prior to the formation of bainitic cementite. The fact that, at the temperature of bainite reaction, the redistribution of substitutional alloying elements appears very difficult implies that the rejection of Si from growing cementite is bound to form a kinetic barrier to their further growth [36]. Nevertheless, it seems safer to assume that the overall kinetics of bainite be controlled by that of ferrite, at least for the low, medium carbon steels mostly involved in this article. Actually, the effect of Si on bainite reaction may be well understood by taking the non partitioning, local equilibrium model. Although Si is not a carbide-forming element, the experimental alloys contain other carbide forming elements, i.e., Mn, Cr, Mo, etc. Si was reported to strengthen the solute drag-like effect of these elements [37]. As a whole, Si would decrease the overall reaction kinetics of bainite. Note that this article concentrates mainly on the apparent influence of single alloying elements on the bainite reaction. It is clear that the influence of different alloying elements can not be separated from each other, and it may well arise from the interactions between two or more of them. The influence of the interaction of alloying elements on bainite reactions will be discussed elsewhere.

It is worthwhile to point out that, unlike the shared ledgewise growth mechanism utilized in pearlite

transformation [38, 39], bainite is formed by means of competitive ledgewise mechanism [29]. In this case, if the growth of one component of bainitic structure is retarded, the other component can still keep growing. This does happen in the high Si containing steels, in that it is well known that bainite may be formed free of carbide [40], and be composed only of subunits of bainitic ferrite [41].

3.3. Influence of Mn on bainite reaction

Manganese is one of the most common chemical elements in steels. Only when its concentration is above 0.5 wt% is it regarded as an alloying element. Fig. 5a is part of the CCT diagram containing the bainite transformation region. Compared to Si, Mn has a significant influence on the bainite reaction. As shown in Fig. 5a, the addition of 0.5 wt% Mn would lead to a decrease of about 50°C in bainite start temperature. The BS is plotted versus Mn concentration in Fig. 5b. Both Fig. 5a and b show that, the bainite formation kinetics would be slowed down by increasing Mn concentration. From Fig. 5b, we see that the decrease rate of BS is approximately 110°C per weight percent Mn at cooling rates ranging from 5.1 to 0.013°C. Compared to Fig. 4b, the influence of Mn on BS is ca. 3 times as strong as that of Si. It should be noted that Mn not only decreases the BS temperature but also shifts the whole bainite transformation region to the right-hand side of the CCT diagram. That is, one of the most important roles of Mn is to increase the incubation period of bainite reaction [30]. From Fig. 5a, we see that if Mn concentration reaches 2 wt%, the incubation period of bainite reaction increases to more than 1000 s. This means that in practice probably only a small amount of bainite will be obtained.

Similar to Fig. 4c, Fig. 5c presents transformation lines corresponding to specific driving forces. The BS line lies well below T600 line in the high Mn concentration region but approximately coincides with T600 in the low Mn concentration region. Again, no apparent dependence of BS upon the driving force of Gibbs energy decrease has been implied in Fig. 5c.

Concerning the influence of Mn on the incubation period, it could be attributed to the influence of Mn on the free energy of austenite. As a strong austenite stabilizer, Mn decreases the free energy difference between ferrite and austenite. The decrease in Gibbs energy difference inevitably prolongs the incubation period.

According to the diffusion controlled ledgewise mechanism, the growth kinetics of bainite is an interface migration controlled process. The interface itself is in a local equilibrium state throughout the bainite transformation. The migration of the transformation frontier interface is further determined by a flattening of the carbon concentration peak accompanying the interface. The peak could be flattened in two ways. First is the diffusion of carbon away from the interface towards the austenite matrix, and the second is the formation of carbide near the interface. Considering the first situation, the influence of alloying elements on bainite growth kinetic might partially be attributed to that on the diffusivity of carbon in austenite. As a medium carbide-forming element, Mn will decrease the diffusivity of C in austenite and thus, slow down the growth kinetics of bainitic ferrite. The fact is that the influence of Mn on the diffusivity of C in austenite could not give rise to the strong dependence of BS on Mn concentration.

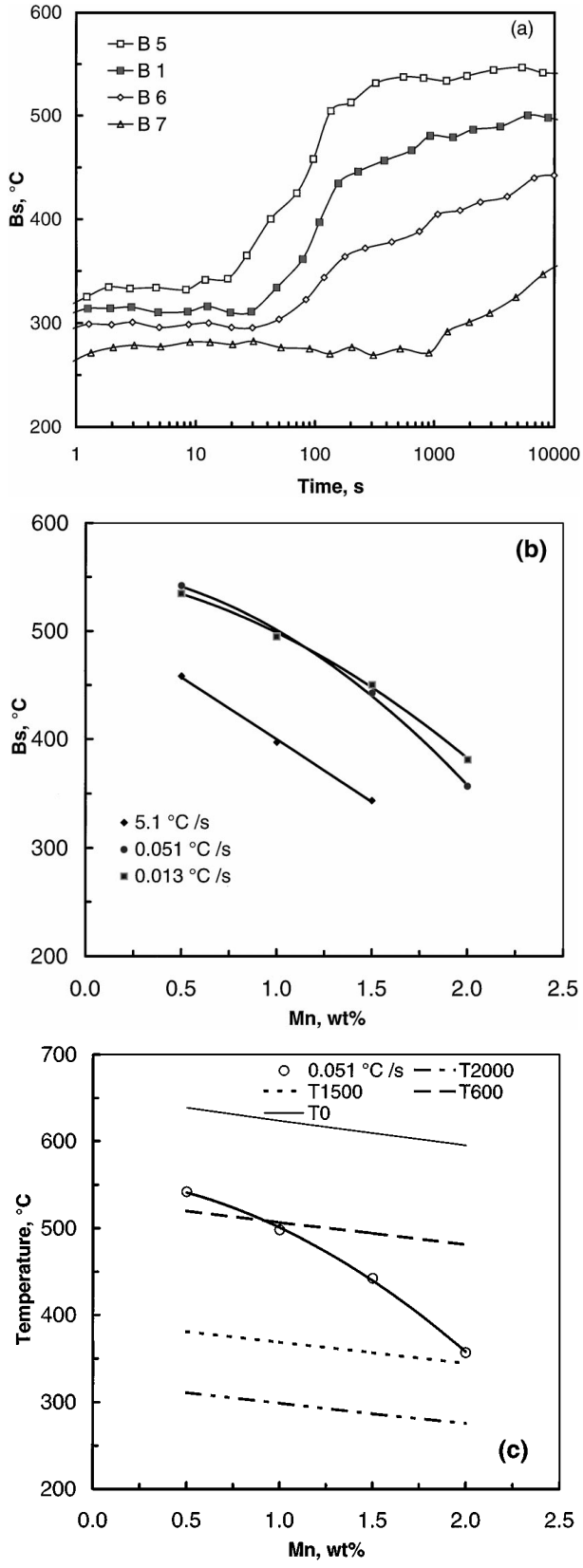

Figure 5 Influence of Mn on bainite start temperature (a) BS versus time; (b) BS versus Mn concentration; (c) compared with thermodynamic calculation.

Alternatively, the influence of Mn on BS could be attributed to the solute drag-like effect. It is immediately evident that the effect of the alloy elements would be rather small if bainite could grow under paraequilibrium conditions. Nevertheless, the interface of ferrite and austenite is supposed to be under local equilibrium with a spike of alloying elements in front of the transformation interface. In this case, the interface turns from true paraequilibrium into NPLE if the width of the spike, defined by D/v is less than atomic dimensions. The transition from paraequilibrium to NPLE will be favored because the mobility of iron or alloy elements inside the interface is higher than in the lattice. The effect of a spike inside the interface depends upon the structure of the interface. In the case of a bainite reaction, the interface is locally ledged and incoherent. The interface migrates by means of individual jumps of atoms across the interface. There should always be enough time for some diffusion of iron and substitutional alloy elements relative to each other within the incoherent interface and the spike can develop there. In the case of martensite transformation, the interface is more coherent, thus the diffusivity inside the interface should be lower and the spike may not develop as well [35]. The effect may be stronger inside the interface by attraction between a carbide-forming element and carbon [42]. This is the very situation for Mn. Mn is a carbide-forming element. The segregation of Mn within the incoherent interface will decrease the activity of C within the interface and the interface itself, and the first one will decrease the driving force for volume diffusion controlled growth kinetics.

3.4. Influence of Cr on bainite reaction

Relative to Mn, Cr is a strong carbide-forming element. Therefore, it is supposed to have a large influence on the formation of bainite. Davenport and Bain were the first to report the strong influence Cr on bainite reaction [43]. The study of the bainite reaction in a pure Fe-C-Cr alloy was made in details by Goldenstein and Aaronson [44]. Unlike the aforementioned, the alloys used in this study contain much more other alloying elements and yet the influence of Cr mentioned later may actually arise from the interaction of all the alloying elements. This is shown in Fig. 6a. Similar to Mn, Cr will decrease the BS temperature and increase the incubation period of bainite reaction. The decrease rate are calculated to be 92 to 133°C for 1 wt% Cr when the cooling rate is within 5.1 to 0.13°C/s. From Fig. 6b, we further see that although the decrease rate of BS is dependent on cooing rate, the linear relationship fits all the curves. It should be pointed out that, though Cr also shifts the bainite region to the right-hand side of a CCT diagram, the shift distance due to Cr is much smaller than that arising from Mn. From Fig. 6a, we know that the position of the bainite nose may shift from 20 s to 100 s by increasing the Cr concentration from 0.5 to 2.0 wt%. In the case of Mn, this shift is from 20 to 1000 s.

Fig. 6c shows the influence of Cr on the Gibbs energy difference between ferrite and austenite. For the Cr concentration involved in this paper, Cr plays a role of a weak austenite stabilizer. As illustrated in Fig. 6c,

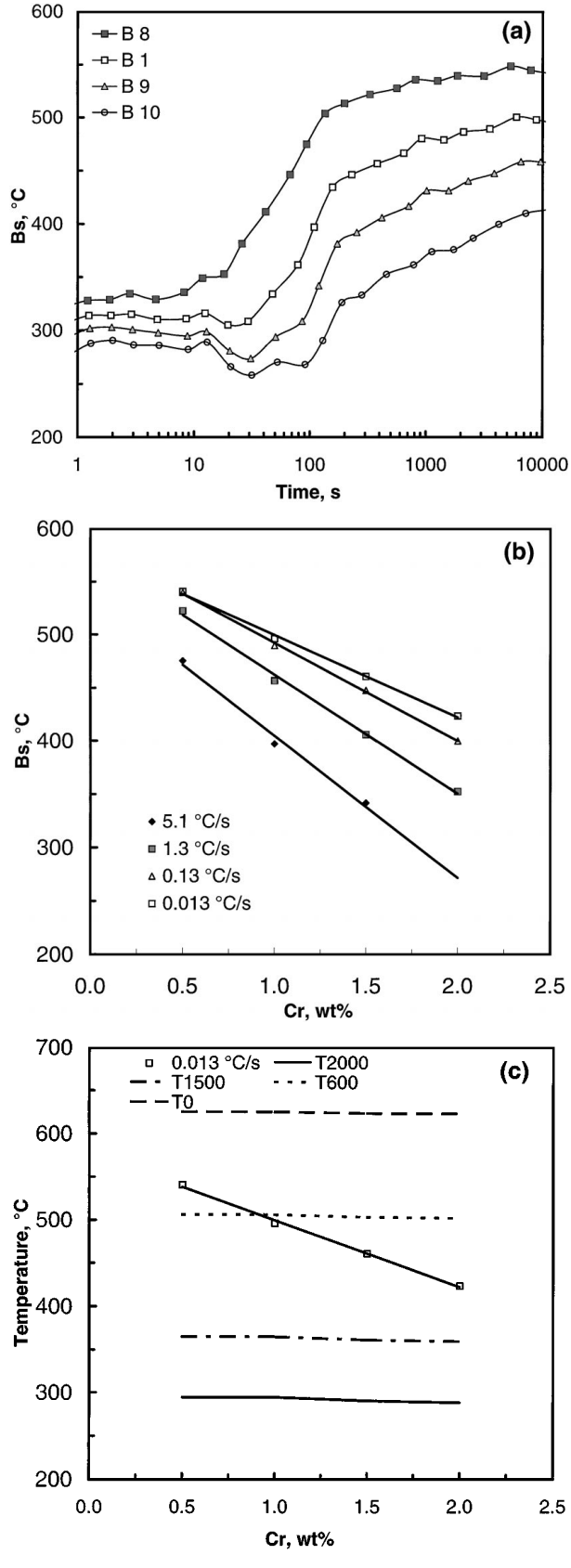

Figure 6 Influence of Cr on bainite start temperature (a) BS versus time; (b) BS versus Cr concentration; (c) compared with thermodynamic calculation.

the lines for specific driving forces are approximately parallel to the x-axis. In contrast to these thermodynamically calculated lines, the BS predicted here is significantly decreased by increasing Cr concentration.

Evidently, the influence of Cr on the BS is similar to that of Mn, and could be well explained with solute

drag-like effect [44]. The difference between the influences of Cr and Mn upon the incubation period of bainite reaction may be attributed to their influence on the Gibbs energy difference. In other words, both the Gibbs energy decrease and the solute-drag effect play an important role in determining the overall kinetics of bainite reaction.

3.5. Influence of Mo on bainite reaction

Mo is the common alloying element used in bainitic steels. Based on the study of the ternary Fe-C-Mo system, Reynolds, *et al.* [45], found that the incomplete character of bainite depends on the combination of C and Mo. The time of transformation stasis increased with the proportion of C and Mo. Regarding the

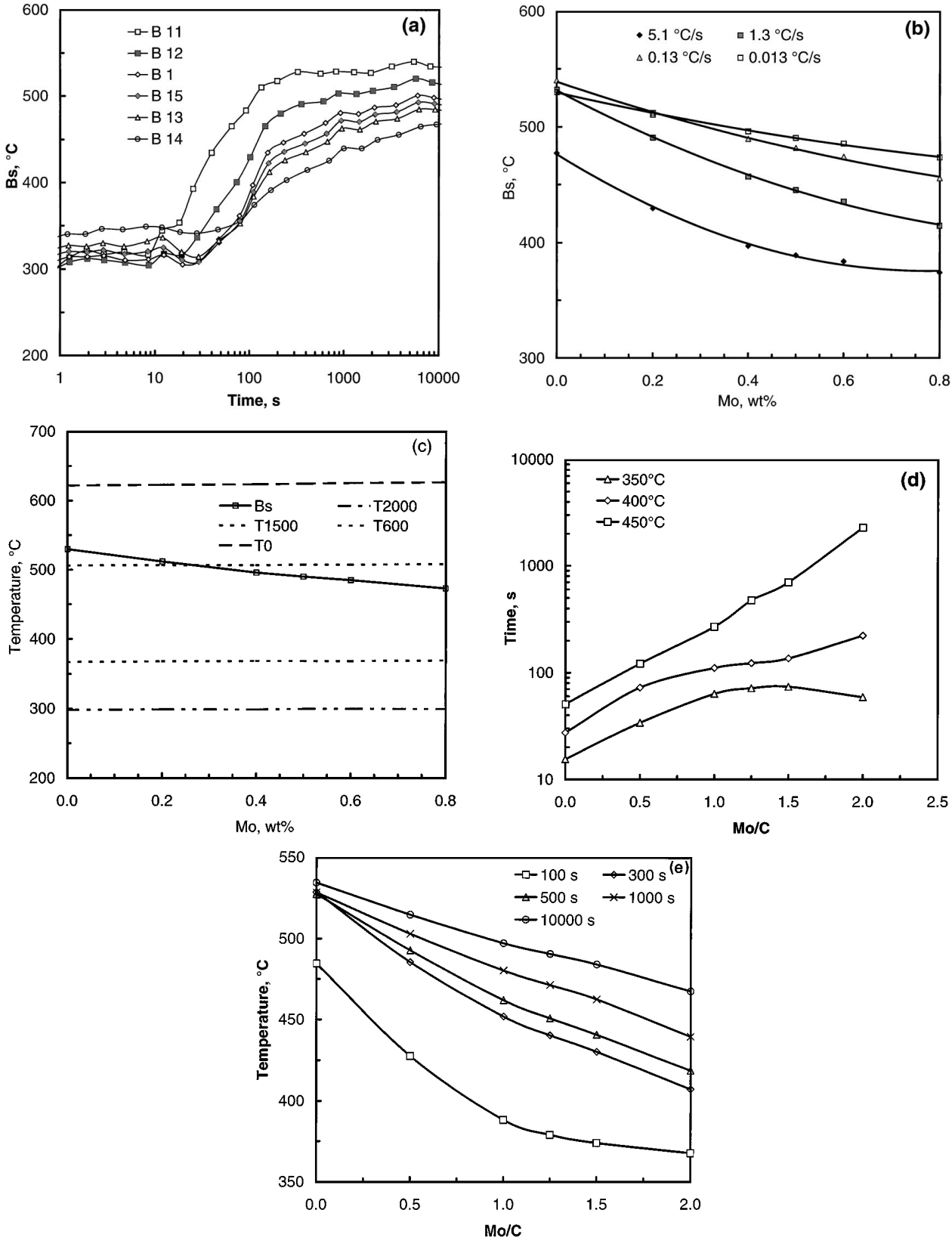

Figure 7 Influence of Mo on bainite start temperature (a) BS versus time; (b) BS versus Mo concentration; (c) compared with thermodynamic calculation, (d) and (e) quasi-isothermal or quasi-isochronal influence of Mo/C proportion.

multicomponent system, it was predicted earlier [46] by a separate ANN model based only on the 64 CCT diagrams from a collection of Vanitec [20] that the end of the bainite formation varies very strongly with the Mo concentration, while the effect of Mo on the bainite start temperature is minimal. This is in agreement with industrial experience. This article, however, will concentrate mainly on the minor dependence of BS upon the Mo concentration. Fig. 7a represents the influence of Mo on the bainite reaction under continuous cooling conditions. It is clear that addition of Mo will decrease the BS temperature, but have a minor influence on the incubation period of bainite reaction. That is, Mo tends to mainly lower, and yet hardly shift the bainite reaction region. Fig. 7b shows the influence of Mo concentration on the BS temperature, for four curves representing four different cooling rates. At a cooling rate of 5.1 and 1.3°C/s, i.e., medium cooling rates, the decrease in BS is approximately linear to the increase in Mo concentration, with a decrease rate equal to 70, and 103°C per 1 wt% Mo, respectively. When the cooling rate is decreased to 0.13°C/s, the dependence of BS on Mo concentration is no longer linear. Another fact is that if Mo < 0.5 wt%, the decrease rate is very high. As a ferrite stabilizer, Mo will increase the driving force of the Gibbs energy difference. This is shown in Fig. 7c, where all calculated lines have slightly positive slopes. However, the predicted BS temperature has a negative slope. Similarly, the NPLE model will give proper explanation for the influence of Mo on bainite reaction kinetics. As reported [44], the SDLE arising from Mo [45] appears to be more effective than that of Cr. This was attributed to the smaller size difference between Cr and Fe. By comparing with the influence of Si, Cr and Mo on the incubation period of bainite reaction, it can be concluded that the incubation time under continuous cooling condition may be determined both by the potential solute drag-like effect of substitutional alloying elements and by the Gibbs energy difference between ferrite and austenite. Fig. 7b also indicates the influence of Mo on MS temperature though this influence is very weak. When the Mo concentration is below 0.5 wt%, MS is independent of Mo, above 0.5%, MS seems to increase slightly with increase of Mo.

Note that CCT actually happens over a certain temperature range, and consequently, any isothermal or isochronal analysis of CCT is physically improper though statistically practicable. Moreover, in the case of CCT, the location of the bainite/austenite boundary actually represents not only the nucleation of bainite but also the growth at its early stage. The isothermal influence of the combination of C and Mo was exhibited in Fig. 7d. At the temperatures of 400 and 450°C, the incubation time of the bainite reaction increases with the proportion of Mo and C, but the increase rate reduces with decreasing temperature. When the temperature is fixed at 350°C, there is a threshold combination of Mo and C, corresponding to Mo concentration of 0.4, above which the incubation time seems independent of the proportion of Mo and C. The isochronal influence of the proportion of Mo and C was given in Fig. 7e. The time of 100 s represents the start part of the sigmoidal curve of bainite reaction, and that of 10000 s falls in full coincidence with the upper limit of BS temperature. The remaining intermediate lines lie in the transient region between the start and stable parts. Except the line of 100 s, all the BS temperatures appear to start from the same point of around 526°C, and then decrease with Mo/C. The larger the fixed incubation time is, the lower the decrease rate is. With respect to the incubation time of 100 s, it seems there is a threshold Mo/C = 1.0, i.e., the Mo concentration of 0.4 wt%; above which the BS temperature keep nearly constant upon increasing Mo/C. The isochronal and isothermal analyses indicate that the proportion of Mo and C has significant influence on the first stage of bainite reaction, which was reported to take place with rapid kinetics, and to be dominated by sympathetic nucleation, although the transformation is presumably initiated by nucleation and growth at the austenite grain boundaries [45]. The larger the proportion is, the lower the BS, and the longer the incubation time.

4. Summary

Influence of single alloying elements of C, Si, Mn, Cr and Mo on bainite reaction under continuous cooling condition in a series of 26 low alloy steels has been predicted by an artificial neural network. Analysis on the predicted results shows that:

1) An increase of carbon concentration will retard the bainite reaction. The decrease rate further depends on the cooling rate and carbon concentration. C also considerably prolongs the incubation period of bainite reaction. The critical driving forces of the test alloys were calculated to be within 150–400 J/mol. The pre-bainite decomposition of austenite also retards the bainite formation and changes the shape of bainite reaction curves. This effect becomes more significant when C concentration is below 0.3 wt%.

2) Alloying elements have a significant influence on the bainite reaction. All the alloying elements studied here tend to decrease the bainite start temperature though degrees of decrease are quite different. For an addition of 1 wt% alloying elements, the decrease rates are 300–600, 100–130, 100–120 and 32 for the elements of C, Cr, Mn and Si. The influence of Mo is very weak and not linear to the Mo concentration. The decrease rates for all alloying elements are further dependent on cooling rates.

3) The incubation period of bainite reaction is affected by alloy elements, but the predicted results show that only Mn tends to shift the nose of bainitic transformation to the far right of the CCT diagram. Thermodynamic analysis indicates that the nucleation of bainite should be thermally activated. Quasi-isochronal and isothermal methods have been employed to analyze the influence of the combination of Mo and C. They indicate that the BS temperature decreases while the incubation period prolongs when the proportion of Mo and C increases. The threshold for the change of both BS and incubation period is Mo/C = 1, corresponding to a Mo concentration of 0.4 wt%.

4) Increases in Mn and Cr concentrations considerably decrease the MS temperature. Si has minor influence on the MS temperature. The influence of Mo, however, depends on the Mo concentration. If Mo < 0.5 wt%, it has minor influence on the MS, whilst above 0.5 wt%, it increases MS temperatures.

5) The dependence of the bainite start conditions on chemical composition, as predicted by the artificial neural network may be used successfully to make a reliable estimate on the physical mechanisms involved in bainite formation for these low alloy lean medium carbon steels.

Acknowledgement

Financial support through the ECSC D3 research program is gratefully acknowledged. One of the authors, Dr. J. Wang would like to express his appreciation to Miss Y. van Leeuwen for assistance in the thermodynamic calculations.

References

1. H. K. D. H. BHADESHIA, *Metal Science* **16** (1982) 159.
2. K. R. KINSMAN, E. EICHEN and H. I. AARONSON, *Metallurgical Transactions A* **6A** (1975) 303.
3. J. S. KIRKALDY, B. A. THOMSON and E. A. BAGANIS, in "Hardenability Concepts with Applications to Steels," edited by D. V. Doane and J. S. Kirkaldy (AIME: Warrendale PA, 1978) p. 82.
4. J. S. KIRKALDY and D. VENUGOPALAN, in "Phase Transformations in Ferrous Alloys," edited by A. R. Marder and J. I. Goldstein (AIME: Warrendale, Pennsylvania, 1984) p. 125.
5. M. ENOMOTO, *ISIJ International* **32** (1992) 297.
6. N. SAUNDERS, A. P. MIODOWNIK and R. W. CAHN, (eds.), CALPHAD Calculation of Phase Diagrams: A Comprehensive Guide. 1998, 1.
7. J. S. KIRKALDY and R. C. SHARMA, *Scripta Metallurgica* **16** (1982) 1193.
8. I. ALEXANDER and H. MORTON, "An Introduction to Neural Computing" (Chapmann & Hall, London, 1993).
9. W. STEVEN and A. G. HAYNES, *JISI* **183** (1956) 349.
10. C. Y. KUNG and J. J. RAYMENT, "Hardenability concepts with applications to steel," Anonymous TMS-AIME, Warrendale, PA, 1978; p. 229.
11. K. W. ANDREWS, *JISI* **203** (1965) 721.
12. R. HECHT-NIELSEN, "Neurocomputing" (Addison-Wesley Publishing Company, Inc. Reading, Massachusetts, 1991).
13. W. G. VERMEULEN, Application of Artificial Neural Networks in Metal Production Processes, 1995.
14. H. K. D. H. BHADESHIA and J. W. CHRISTIAN, *Metall. Trans. A* **21A**(4) (1990) 767.
15. T. KO and A. M. COTTRELL, *JISI* **172** (1952) 307.
16. F. R. HEHEMANN, K. R. KINSMAN and H. I. AARONSON, *Metall. Trans.* **3** (1972) 1077.
17. D. E. COATES, *ibid.* **4** (1973) 2313.
18. R. W. KENNARD and L. A. STONE, *Technometrics* **11** (1969) 137.
19. W. W. CIAS, Climax Molybdenum Company, Greenwich, 1973.
20. G. F. VAN DER VOORT, ASM International, Reading PA, 1991.
21. C. DORREPAAL, Modelling of CCT Diagrams Using Artificial Neural Networks. 1997, Delft University of Technology. Master.
22. J. WANG, P. VAN DER WOLK and S. VAN DER ZWAAG, *ISIJ International* **39**(10) (1999) 1038.
23. Y. OHMORI and T. MAKI, *Mat. Trans. JIM* **32** (1991) 631.
24. J. W. CHRISTIAN, Proc. ICOMAT-79, Anonymous MIT Press, Cambridge, MA, 1979, p. 220.
25. L. KAUFMAN, S. V. RADCLIFFE and M. COHEN, in "Decomposition of Austenite by Diffusional Processes," edited by V. F. Zackay and H. I. Aaronson (Interscience, 1962) p. 313.
26. L. KAUFMAN and M. COHEN, *Prog. Metal Physics* **1** (1958) 165.
27. C. L. MAGEE, "Phase Transformations" (ASM, 1970) p. 115.
28. M. HILLERT, *Acta Metallurgica* **1** (1953) 764.
29. H. I. AARONSON, W. T. J. REYNOLDS, G. J. SHIFLET and G. SPANOS, *Metall. Trans. A* **21A**(6) (1990) 1343.
30. S. K. LIU, L. YANG, D. G. ZHU and J. ZHANG, *Metall. Mat. Trans. A* **25A** (1994) 1991.
31. G. B. OLSON and M. COHEN, *Metallurgical Transactions A* **7A** (1976) 1905.
32. *Idem., ibid.* **7A** (1976) 1897.
33. J. WANG, P. VAN DER WOLK and S. VAN DER ZWAAG, EuroMat'99, Sep. 27–30, 1999, Munich, Germany.
34. H. FANG, J. WANG and Y. ZHENG, *Metall. Mat. Trans. A* **25A**(9) (1994) 2001.
35. M. HILLERT, *ibid.* **25A**(9) (1994) 1957.
36. S. J. BARNARD, G. D. W. SMITH, A. J. GARRATT-REED and J. VANDER SANDE, in "Solid-Solid Phase Transformations," edited by H. I. Aaronson, D. E. Laughlin, R. F. Sekerka and C. M. Wayman (Metallurgical Society of AIME, 345 Est 47th Street, New York, NY 10017, USA, 1982) p. 881.
37. S. K. LIU and J. ZHANG, *Metall. Trans. A* **21A** (1990) 1517.
38. S. A. HACKNEY and G. J. SHIFLET, in "Phase Transformations in Ferrous Alloys," edited by A. R. Marder and J. I. Goldstein (AIME, Warrendale, Pennsylvania, 1984) p. 237.
39. *Idem., Acta Metallurgica* **35** (1987) 1007.
40. B. P. J. SANDVIK, *Metallurgical Transactions A* **13A** (1982) 777.
41. J. WANG, H. FANG, Z. YANG and Y. ZHENG, *ISIJ International* **35**(8) (1995) 992.
42. K. R. KINSMAN and H. I. AARONSON, "Transformation and Hardenability in Steels" (Climax Molybdenum Co., Ann Arbor, Michigan, 1967) p. 39.
43. E. S. DAVENPORT and E. C. BAIN, *Trans. AIME* **90** (1930) 117.
44. H. GOLDENSTEIN and H. I. AARONSON, *Metall. Trans. A* **21A** (1990) 1465.
45. W. T. REYNOLDS, JR., F. Z. LI, C. K. SHUI and H. I. RONSON, *ibid.* **21A** (1990) 1433.
46. P. J. VAN DER WOLK, W. G. VERMEULEN and S. VAN DER ZWAAG, 2nd International Conference on Modelling of Metal Rolling Processes, edited by J. H. Beynon (The Institute of Materials, London, 1996) p. 378.

Received 13 May 1999
and accepted 3 February 2000